ARTICLE

Density Functional Study on Structures and Relative Stability of $Gd(H_2O)_n^{3+}$ (n=8,9)

Wei Xiao[a], Qiong-qiong Xia[a], Yong-fan Zhang[b], Li-xin Ning[a*], Zhi-feng Cui[a]

a. Department of Physics, Anhui Normal University, Wuhu 241000, China
b. Department of Chemistry, Fuzhou University, Fuzhou 350002, China

(Dated: Received on April 13, 2009; Accepted on May 6, 2009)

Density functional theory calculations were performed to study the structures and relative stability of the gadolinium complexes, $Gd(H_2O)_n^{3+}$ (n=8,9), *in vacuo* and in aqueous solution. The polarizable continuum model with various radii for the solute cavity was used to study the relative stability in aqueous solution. The calculated molecular geometries for n=8 and 9 obtained *in vacuo* are consistent with those observed in experiments. It was found that while the nona-aqua complex is favored in the gas phase, in aqueous solution the octa-aqua conformation is preferred. This result, independent of the types of cavities employed, is in agreement with the experimental observation. The reliability of the present calculation was also addressed by comparing the calculated and experimental free energy of hydration, which revealed that the UA0, UAHF, and UAKS cavities are most appropriate when only the first solvation shell is treated explicitly.

Key words: Density functional theory, Gadolinium hydrate, Relative stability, Polarizable continuum model, Solute cavity

I. INTRODUCTION

Compounds of gadolinium(III) have attracted considerable attention due to their potential applications as contrast agents for magnetic resonance imaging (MRI) in clinical diagnostics and biomedical research [1]. As the bare Gd^{3+} is toxic, complexation with polydentate ligand to form compounds of high kinetic and thermodynamic stability in solution is required for *in vivo* application. The resulting complexes usually have one or more water molecules coordinated to the ion. This fact is relevant for the complex used as MRI contrast agent, since the ability of the complex to enhance the image contrast is related to its relaxivity. The relaxivity can be affected by the chemical exchange between water molecules in the first solvation shell and the bulk solvent. In addition, mechanisms of binding between Gd^{3+} and chelate ligands can be significantly influenced by the strength of Gd-OH_2 interaction and the water coordination around the ion. Therefore, knowledge of interaction between Gd^{3+} and the ligating water molecules is imperative, which, among other reasons, drives research on structural and thermodynamic properties of gadolinium aqua complexes.

The first coordination sphere of Gd^{3+} in aqueous solution is known to be dynamic, because the ion-dipole interaction results in fast water exchange between the hydration layer and bulk water. Experimental studies by extended X-ray absorption fine structure (EXAFS) and X-ray diffraction methods give a hydration number of between 7.5 and 9.9 [2]. Later, neutron diffraction experiments on lanthanide solutions [3] revealed that the Gd^{3+} forms an octa-aqua complex with a square antiprismatic (SAP) geometry. By contrast, Gd^{3+} is 9-coordinated in the solid state with a tricapped trigonal prismatic (TCTP) geometry, although structural differences exist depending on the counter-ion in the crystal [4,5]. From a theoretical point of view, the hydrated Gd^{3+} has been investigated by Clavaguéra *et al.* based on molecular dynamics simulations including many-body polarization effects [6]. The results showed an equilibrium coordination of between nine- and eightfold for Gd^{3+} in liquid water, with the former being preferred and the latter as an intermediate species. Using first principles molecular dynamics Yazyev and Helm reported, however, an observation that the first coordination shell contains eight water molecules with an average arrangement close to the SAP geometry [7]. From these studies we can see that further theoretical work is needed, particularly with respect to the coordination of water molecules in the inner sphere around the ion.

Ab initio calculations on lanthanide complexes have been quite a computational challenge due to the large number of electrons in the lanthanide ion with large relativistic and correlation effects [8]. Recently, Dinescu *et al.* have investigated the structural and thermodynamic properties of $Ce(H_2O)_{8,9}^{3+}$ by density functional

*Author to whom correspondence should be addressed. E-mail: ninglx@mail.ahnu.edu.cn

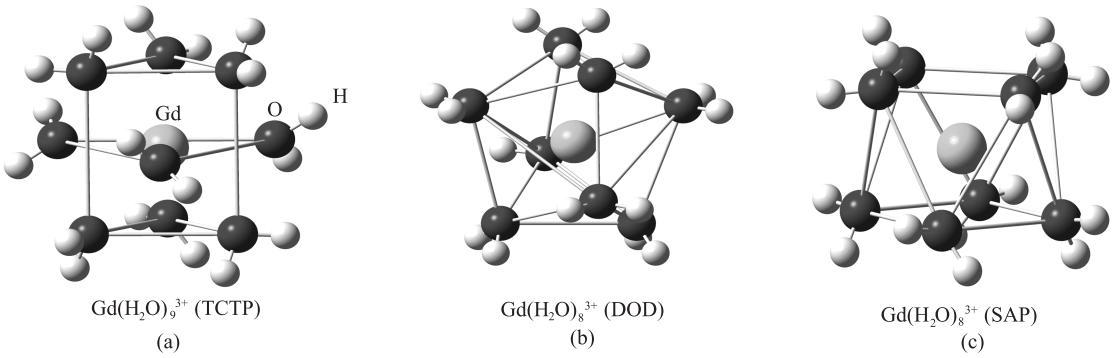

$Gd(H_2O)_9^{3+}$ (TCTP) (a)

$Gd(H_2O)_8^{3+}$ (DOD) (b)

$Gd(H_2O)_8^{3+}$ (SAP) (c)

FIG. 1 Optimized structures of $Gd(H_2O)_n^{3+}$ (n=8, 9) using DFT.

theory (DFT) [9]. The nature of the open 4f subshell (Ce^{3+} $4f^1$) was also examined with the complete active space self-consistent field (CASSCF) method, showing that the open-shell nature can be described well by the single-determinant formalism as implemented in DFT [9]. For $Gd(H_2O)_{8,9}^{3+}$ under study, the single-determinant description is not a problem, since the half-filled 4f subshell ($4f^7$) of Gd^{3+} gives rise to a $^8S_7$ ground state and the first excited $^7P_{7/2}$ state was experimentally observed to be about 4 eV above [10]. In this work, using DFT, we studied the structures and relative stability of $Gd(H_2O)_n^{3+}$(n=8,9) *in vacuo* and in aqueous solution. For the latter case, the first hydration shell is described by means of a proper cluster of water molecules, and interactions with the bulk water are simulated using the PCM model.

II. COMPUTATIONAL METHODS

The calculations were performed using the hybrid B3LYP density functional [11,12] as implemented in the Gaussian 03 suite of programs [13]. It has been shown that hybrid functionals are the most accurate functionals available as far as energetics is concerned [14] and they are often the method of choice within computational lanthanide chemistry [9,15,16]. The 6-31++G(d,p) basis sets were used for the coordinated water molecules, whereas for gadolinium ion, the relativistic effective core potential (RECP) of CEP-31G coupled with the optimized [4s4p2d2f]-GTO valence basis set was employed [17]. This RECP treats [Kr]$4d^{10}$ as fixed cores, and the $5s^25p^64f^75d^16s^2$ shells (18 electrons) are taken into account explicitly. This choice of the RECP and basis sets is based on the ability to reproduce reliably experimental molecular geometries, vibrational spectra, and magnetic coupling of gadolinium compounds [18,19]. The optimized structures were confirmed by the frequency calculation at the same level to be the real minimum without any imaginary vibration frequency. The convergence criterion for energy was set at 10^{-8} a.u. and fine numerical integration grids (IntGrid=Ultrafine) were used throughout the calculation.

To examine the accuracy of the theoretical level adopted in this work, we have, in fact, calculated the equilibrium structure and stabilization energy of $Gd(H_2O)^{3+}$ using various density functionals as implemented in the program. The basis set superposition error (BSSE) as a result of incompleteness of the basis sets was corrected with the commonly used counterpoise correction [20]. The method was applied as a single-point correction to the optimized geometry. The results were compared with those reported from the Dirac-Hartree-Fock (DHF) based relativistic second-order Møller-Plesset perturbation (RMP2) calculations [21], showing that the Gd−O bond length of 2.214 Å and the stabilization energy of 4.573 eV from the B3LYP calculations are among those closest to the RMP2 values of 2.17 Å and 4.7 eV, respectively. This comparison indicates that the employed level of theory could be adequate to provide reliable information on structures and energetics for the nona- and octa-aqua Gd^{3+} complexes of interest here.

III. RESULTS AND DISCUSSION

A. Nuclear geometries

For $Gd(H_2O)_9^{3+}$, a starting TCTP structure with ideal D_{3h} symmetry was considered for geometry optimization. Without symmetry constraints, the optimization provides a slightly distorted TCTP geometry (C_1 symmetry), with the symmetry being D_3 when the position tolerance is 0.1 Å; see Fig.1(a). The calculated average Gd−O bond length for the prismatic bond is 2.512 Å, whereas for the equatorial bond the length is 2.542 Å. The slightly larger value of the equatorial bond length relative to that of the prismatic one is due to the fact that the equatorial ligating water molecules experience an excess steric repulsion, which is alleviated by an increase in the Gd−O bond lengths [22]. Experimentally, this bond lengthening has been observed in solid-state lanthanide hydrates which all present a

DOI:10.1088/1674-0068/22/04/395-400

TABLE I Calculated electronic properties of the optimized $Gd(H_2O)_n^{3+}$ (n=8,9) complexes from the natural population analysis.

		Magnetic moment/μ_B	Natural electronic configuration	Natural charge
$Gd(H_2O)_9^{3+}$ (TCTP)	Gd	6.99	$4f^{7.01}5d^{0.11}6s^{0.15}$	2.73
	O	0.00	$2s^{1.75}\ 2p^{5.32}\ 3p^{0.01}$	−1.08
	H	0.00	$1s^{0.44}$	0.56
$Gd(H_2O)_8^{3+}$ (SAP)	Gd	6.99	$4f^{7.01}5d^{0.12}\ 6s^{0.15}$	2.72
	O	0.00	$2s^{1.75}2p^{5.33}3p^{0.01}$	−1.07
	H	0.00	$1s^{0.44}$	0.56
$Gd(H_2O)_8^{3+}$ (DOD)	Gd	6.99	$4f^{7.01}5d^{0.11}6s^{0.15}$	2.73
	O	0.00	$2s^{1.75}2p^{5.32}3p^{0.01}$	−1.08
	H	0.00	$1s^{0.44}$	0.56

TCTP geometry around the ion from X-ray and neutron diffraction measurements [23]. Although the coordination geometries of these hydrates are similar, structural differences exist depending on the counter-ion in the crystal, which have been attributed to hydrogen-bonding networks between the counter-ion and coordinated water molecules [24]. With ethylsulfate and triflate as counter-ions, the nona-aqua Gd^{3+} with TCTP structure of C_{3h} symmetry was observed in the solid state. The measured prismatic and equatorial bond lengths were 2.401 and 2.536 Å, respectively, in the former case [4], and 2.395 and 2.536 Å, respectively, in the latter case [5]. While our predicted bond lengths for the equatorial ligating waters are in good agreement with the solid state structure, the calculated lengthening of the equatorial bonds (by 0.03 Å) is much smaller than the experimental observations (∼0.14 Å). This is not entirely unexpected since the calculated values refer to an isolated molecule in the gas phase. In the condensed phase, the Gd−O bonds should shorten on the basis of solvation effects, for example, the crystal packing forces and/or hydrogen bonding.

For $Gd(H_2O)_8^{3+}$, two different ideal structures were initially considered: a dodecahedral (DOD) structure of D_{2d} symmetry and an SAP structure of D_{4d} symmetry. After geometry optimization, we obtained a D_{2d} symmetry for the optimized DOD structure (Fig.1(b)) and a C_4 symmetry for the optimized SAP one (Fig.1(c)), the latter being 77.940 kJ/mol lower in energy than the former. It should be mentioned that the SAP geometry has been observed in the structure determined for Gd^{3+} in aqueous solution [3]. The calculated average Gd−O bond length for the DOD structure is 2.505 Å, while for the SAP structure the length is 2.478 Å. Experimentally, the average Gd−O bond length for Gd^{3+} in aqueous solutions was determined to be 2.37−2.41 Å obtained by EXAFS and X-ray diffraction methods [2], and 2.40±0.05 Å from electron nucleus double resonance measurements [25,26]. The overestimation of the calculated Gd−O bond length may presumably be due to the fact that only the first hydration shell was included in our calculations. It is expected that this discrepancy would be alleviated if second-shell waters were included in the geometry optimization. Such work is in progress. Finally, we note that, by comparing the optimized octa-aqua SAP and nona-aqua TCTP structures, the increase of the hydration number from eight to nine results in a Gd−O bond elongation of about 0.05 Å on average, indicating an excess of steric repulsion experienced by the water molecules in the latter case.

B. Population analysis

Population analyses are common ways to characterize qualitatively the electronic structure of metal atoms. It has been shown that the natural population analysis [27] is generally more suitable than the standard Mulliken population analysis for 4f-block elements [28]. A natural population analysis was thus carried out for the ground states of the geometry-optimized $Gd(H_2O)_9^{3+}$ and $Gd(H_2O)_8^{3+}$ systems. The resulting magnetic moments, electronic configurations, and natural charges on Gd, O, and H atoms are collected in Table I. The results for the three systems show that the magnetic moment on Gd atoms are all equal to 6.99 μ_B, which is compatible with a spin of 7/2 that would result from Hund's rule for the half-filled 4f subshell configuration. Therefore, a localized picture for the 4f spin moment could be envisaged. The electron configurations for Gd, O, and H atoms as derived from the analysis are almost identical in all the three cases. One can see that the occupation number (7.01 electrons) of Gd 4f orbitals is nearly equal to the number of the isolated $Gd^{3+}(4f^7)$, indicating the very small participation of 4f orbitals in bonding. The Gd 5d and 6s occupations in Table I indicate the presence of small covalent Gd−O bonding from these two types of orbitals, because the occupations deviate from a purely ionic bonding between $Gd^{3+}(4f^7)$ and H_2O molecules. The natural charges resulting from these electronic configurations are also listed in Table I, from which it is seen that an average of 2.73 electrons per Gd atom is transferred to the ligating waters.

DOI:10.1088/1674-0068/22/04/395-400

TABLE II Thermodynamic properties for reaction (1) at T=298.15 K and P=10^5 Pa, $\Delta G_{\rm gas}$(corr)=−39.75 kJ/mol, $\Delta G_{\rm SS}$=−7.95 kJ/mol, and the other Gibb free energies are in unit of kJ/mol.

PCM cavity	$\Delta\Delta G_{\rm sol}$(elec)	$\Delta\Delta G_{\rm sol}$(nonelec)	$\Delta\Delta G_{\rm sol}$(tot)	$\Delta G_{\rm sol}$(corr)	$V_{\rm cavity}$/Å^3	
					$Gd(H_2O)_9{}^{3+}$	$Gd(H_2O)_8{}^{3+}$
UA0	71.34	−11.09	60.25	12.55	240.44	221.05
UAHF/UAKS	60.12	−4.81	55.31	7.61	253.96	237.46
UFF	70.00	−7.91	62.09	14.39	271.79	247.19
Pauling	101.21	10.33	111.54	63.84	212.08	190.12

C. Relative stability

1. Gas phase results

The relative stability between the nona- and octa-aqua Gd^{3+} ions were determined by calculating the free energy variation (ΔG) of the reaction

$$Gd(H_2O)_8{}^{3+} + H_2O \xrightarrow{\Delta G} Gd(H_2O)_9{}^{3+} \quad (1)$$

$$\Delta G = G[Gd(H_2O)_9{}^{3+}] - G[Gd(H_2O)_8{}^{3+}] - G[H_2O] \quad (2)$$

In the above two equations, $Gd(H_2O)_8{}^{3+}$ refers to the optimized SAP structure, as it is more stable than the DOD structure (by 77.940 kJ/mol). To assess whether $Gd(H_2O)_9{}^{3+}$ or $Gd(H_2O)_8{}^{3+}$ is preferred energetically, we first investigated the gaseous energetics of reaction (1). The electronic energy ($\Delta E_{\rm elec}$), $\Delta E_{\rm ZPE}$, enthalpy ($\Delta H_{\rm gas}$), and Gibbs free energy ($\Delta G_{\rm gas}$) for this reaction are −94.39, −84.77, −86.78, and −47.07 kJ/mol, respectively. It shows that the nona-hydrated arrangement is more favored over the octa-hydrated one by −47.07 kJ/mol. It should be noted that the calculation of energetics for reaction (1) is subject to BSSE. This error was estimated based on the previously optimized TCTP geometry of $Gd(H_2O)_9{}^{3+}$ using the scheme by Xantheas [29]. In the BSSE estimation, the two fragments specified are the ligating water molecule with the longest Gd−O bond distance and the remaining $Gd(H_2O)_8{}^{3+}$ structure. The computed BSSE magnitude for the electronic energy of reaction (1) is 7.32 kJ/mol, and the BSSE-corrected free energy variation ($\Delta G_{\rm gas}$(corr)=−39.75 kJ/mol).

2. Solvent phase results

To investigate the relative stability of $Gd(H_2O)_n{}^{3+}$ (n=8, 9) in aqueous solution, the PCM model with different implementations was employed to account for the interaction between the Gd^{3+} complexes and the liquid water. We note that there are few PCM studies reported in the literature on 4f-complexes [8,9,30]. The free-energy variation ($\Delta G_{\rm sol}$(corr)) of reaction (1) in the solvent phase may be written as

$$\Delta G_{\rm sol}(\text{corr}) = \Delta G_{\rm gas}(\text{corr}) + \Delta\Delta G_{\rm sol}(\text{tot}) + \Delta G_{\rm SS} \quad (3)$$

where $\Delta\Delta G_{\rm sol}$(tot) is the total solvation contribution to the free energy variation. $\Delta G_{\rm SS}$ is the standard-state thermodynamic correction for the reaction due to the different standard concentrations of solution and gas phase, and is equal to $-RT\ln 24.5$, where R is the gas constant and T=298.15 K [31]. Within the PCM model, the solvation contribution $\Delta\Delta G_{\rm sol}$(tot) can be expressed as

$$\Delta\Delta G_{\rm sol}(\text{tot}) = \Delta\Delta G_{\rm sol}(\text{elec}) + \Delta\Delta G_{\rm sol}(\text{nonelec}) \quad (4)$$

$$\Delta\Delta G_{\rm sol} = \Delta G_{\rm sol}[Gd(H_2O)_9{}^{3+}] - \Delta G_{\rm sol}[Gd(H_2O)_8{}^{3+}] - \Delta G_{\rm sol}(H_2O) \quad (5)$$

Various contributions to the free energy variation of reaction (1) for the solute cavity models used are reported in Table II. It is interesting to see that, although the gas-phase calculations predict the nona-hydrated $Gd(H_2O)_9{}^{3+}$ to be more stable, the PCM calculations with all types of cavity employed give the octa-hydrated $Gd(H_2O)_8{}^{3+}$ as the favorable one, in agreement with the observation from neutron diffraction experiments [3]. In all these cases, the positive sign of the solvation contribution $\Delta\Delta G_{\rm sol}$(tot) changes the free energy variation from negative value in the gas phase to positive values in aqueous solution, that is, alter reaction (1) from exergonic to the experimentally known endergonic [3]. These results highlight the importance of solvent effects in the prediction of the energetic preference for gadolinium hydrates.

As listed in Table II, the calculated values for the free-energy variation span a wide range from 7.61 kJ/mol to 63.84 kJ/mol. This observation suggests that PCM corrections are highly dependent on the choice of solute cavity. The results are identical for UAHF and UAKS radii due to their identical cavity sizes (see the last two columns of Table II). As expected, the cavities with larger sizes (comparing UA0, UAHF/UAKS, and UFF with Pauling) generally give smaller positive $\Delta\Delta G_{\rm sol}$(tot) (and thus $\Delta G_{\rm sol}$(corr)) values. An exception is the UFF cavity, which, although having the largest size, does not yield the smallest $\Delta\Delta G_{\rm sol}$(tot). This indicates that the cavity shape chosen may also be important in the PCM calculations.

3. Standard hydration free energies

As shown above, the calculated $\Delta G_{\rm sol}$(corr) value exhibits a strong dependence on the type of cavity

DOI:10.1088/1674-0068/22/04/395-400

TABLE III Thermodynamic properties for reaction (2) at T=298.15 K and P=10^5 Pa, $\Delta G_{\rm gas}$(corr)=−1799.20 kJ/mol, $\Delta G_{\rm SS}$=−7.95 kJ/mol, and the other Gibb free energies are in unit of kJ/mol.

PCM cavity	$\Delta\Delta G_{\rm sol}$(elec)	$\Delta\Delta G_{\rm sol}$(nonelec)	$\Delta\Delta G_{\rm sol}$(tot)	$\Delta G_{\rm sol}$(corr)
UA0	−1581.80	−14.06	−1595.86	−3403.01
UAHF/UAKS	−1540.26	−8.66	−1548.92	−3356.07
UFF	−1445.40	25.98	−1419.42	−3226.57
Pauling	−1534.94	37.95	−1496.99	−3304.14

with the PCM framework. In the following, we examine the performance of the cavities chosen in this work by comparing the calculated standard hydration free energy ($\Delta G^{\ominus}_{\rm hyd}$) against experiment. Direct experimental determination of the $\Delta G^{\ominus}_{\rm hyd}$ values is not feasible, and they are usually calculated indirectly using semi-empirical methods (Born-Haber thermochemical cycles). In the case of the Gd^{3+} aqua ion, Bratsch and Lagowski reported a free energy of hydration from −3467.03 kJ/mol to −3374.98 kJ/mol at 298.15 K [20,32]. It has been shown that the hydration free energy of an ion can be accurately predicted when the first solvation shell is treated quantum mechanically and the solvent effect simulated using a continuum model [30]. On the basis of these considerations, we have analyzed the solvent effects on the free energy of hydration of Gd^{3+} by including eight water molecules in the first solvation shell and approximating the solvent by the PCM model. Within such a mixed solvation model, the $\Delta G^{\ominus}_{\rm hyd}$ corresponds to the free energy variation ($\Delta G_{\rm sol}$(corr)) of the following reaction:

$$Gd^{3+}(\text{gas}) + (H_2O)_8(\text{aq}) \rightarrow Gd(H_2O)_8{}^{3+}(\text{aq}) \quad (6)$$

The results for the above reaction are reported in Table III, which shows that the hydration values calculated with UA0 and UAHF/UAKS cavities agree well with the experimental result from −3467.03 kJ/mol to −3374.98 kJ/mol [20,32]. The UA0 cavity reproduces the experimental value to within 17 kJ/mol, while the UAHF/UAKS cavities yield a value reasonably close to the experimental one (within 63 kJ/mol). These results suggest that cavities generated with the UA0, UAHF, and UAKS radii in the PCM method are most appropriate for the Gd^{3+} aqua ion when only the primary hydration shell is treated explicitly in the calculation.

IV. CONCLUSION

We investigated the structures and relative stability of Gd^{3+} aqua complexes *in vacuo* and in aqueous solution using DFT. Full optimization of structures *in vacuo* reveals that the calculated nona-hydrated $Gd(H_2O)_9{}^{3+}$ adopts a TCTP geometry consistent with the experimental solid-state structures, while the calculated octa-hydrated $Gd(H_2O)_8{}^{3+}$ has a stable SAP geometry consistent with that observed in aqueous solution. Calculations of thermodynamic features, based on the optimized structures and the PCM model for the solvent effect, show that $Gd(H_2O)_9{}^{3+}$ is preferred energetically over $Gd(H_2O)_8{}^{3+}$ in the gas phase, while in the solution phase the reverse is true. This latter result agrees well with experimental findings, and is independent of the types of cavities used in the PCM calculations. Finally, the performance of cavity models, within the context of the present level of theory, was evaluated against the experimental free energy of hydration of Gd^{3+}. It was found that the cavities generated with the UA0, UAHF, and UAKS radii are most appropriate when only the primary solvation shell is taken into account explicitly. The present study highlights the importance of the solvent effects in the study of energetics for Gd^{3+} in aqueous solution.

V. ACKNOWLEDGMENTS

This work was supported by the National Natural Science Foundation of China (No.10804001, No.10674002, and No.20773024), the National High Technology Research and Development Program of China (No.2006AA09Z243-3), and the Program for Innovative Research Team in Anhui Normal University of China.

[1] A. E. Merbach and É. Tóth, *The Chemistry of Contrast Agents in Medical Magnetic Resonance Imaging*, Chichester, UK: Wiley, (2001).
[2] H. Ohtaki and T. Radnai, Chem. Rev. **93**, 1157 (1993).
[3] C. Cossy, L. Helm, D. H. Powell, and A. E. Merbach, New J. Chem. **19**, 27 (1995).
[4] R. E. Gerkin and W. J. Reppart, Acta Cryst. C **40**, 781 (1984).
[5] A. Chatterjee, E. N. Maslen, and K. J. Watson, Acta Cryst. B **44**, 381 (1988).
[6] C. Clavaguéra, F. Calvo, and J. P. Dognon, J. Chem. Phys. **124**, 074505 (2006).
[7] O. V. Yazyev and L. Helm, J. Chem. Phys. **127**, 084506 (2007).
[8] U. Cosentino, A. Villa, D. Pitea, G. Moro, and V. Barone, J. Phys. Chem. B **104**, 8001 (2000).
[9] A. Dinescu and A. E. Clark, J. Phys. Chem. A **112**, 11198 (2008).

DOI:10.1088/1674-0068/22/04/395-400

[10] W. C. Martin, R. Zalubas, and L. Hagan, *Atomic Energy levels-The Rare Earth Elements, National Bureau of Standards Reference Data, Series 60*, Washington: US Department of Commerce, (1978).
[11] D. Becke, J. Chem. Phys. **98**, 5648 (1993).
[12] C. Lee, W. Yang, and R. G. Parr, Phys. Rev. B **37**, 785 (1988).
[13] M. J. Frisch, G. W. Trucks, H. B. Schlegel, G. E. Scuseria, M. A. Robb, J. R. Cheeseman, V. G. Zakrzewski, J. A. Montgomery, R. E. Stratmann, J. C. Burant, S. Dapprich, J. M. Daniels, K. N. Kudin, M. C. Strain, O. Farkas, J. Tomasi, V. Barone, M. Cossi, R. Cammi, B. Mennucci, C. Pomelli, C, Adamo, S. Clifford, J. Ochterski, G. A. Petersson, P. Y. Ayala, Q. Cui, K. Morokuma, N. Rega, P. Salvador, J. J. Dannenberg, D. K. Malick, A. D. Rabuck, K. Raghavachari, J. B. Foresman, J. Cioslowski, J. V. Ortiz, A. G. Baboul, B. B. Stefanov, G. Liu, A. Liashenko, P. Piskorz, I. Komaromi, R. Gomperts, R. L. Martin, D. J. Fox, T. Keith, M. A. Al-Laham, C. Y. Peng, A. Nanayakkara, M. Challacombe, P. M, W. Gill, B. Johnson, W. Chen, M. W. Wong, J. L. Andres, C. Gonzalez, M. Head-Gordon, E. S. Replogle, and J. A. Pople, *Gaussian 03, Revision B.05,* Pittsburgh, PA: Gaussian, Inc., (2003).
[14] R. L. Martin, *Electronic Structure: Basic Theory and Practical Methods*, Cambridge UK: Cambridge University Press, 152 (2004).
[15] L. Maron and O. Eisenstein, J. Phys. Chem. A **104**, 7140 (2000).
[16] P. J. Hay, R. L. Martin, J. Uddin, and G. E. Scuseria, J. Chem. Phys. **125**, 034712 (2006).
[17] T. R. Cundari and W. J. Stevens, J. Chem. Phys. **98**, 5555 (1993).
[18] C. Adamo and V. Barone, J. Comput. Chem. **21**, 1153 (2000).
[19] L. X. Ning, Y. F. Zhang, Z. F. Cui, M. I. Trioni, and G. P. Brivio, J. Phys. Chem. A **112**, 13650 (2008).
[20] S. F. Boys and F. Bernardi, Mol. Phys. **19**, 553 (1970).
[21] Y. Mochizuki and H. Tatewaki, Chem. Phys. **273**, 135 (2001).
[22] E. N. Rizkalla and G. R. Choppin, *Handbook on the Physics and Chemistry of Rare Earths*, K. A. Gschneider, Jr. and L. Eyring, Eds., Amsterdam: Elsevier, 393 (1991).
[23] E. N. Rizkalla and G. R. Choppin, *Handbook on the Physics and Chemistry of Rare Earths*, K. A. Gschneider, Jr. and L. Eyring, Eds., Amsterdam: Elsevier, 529 (1994).
[24] J. McB. Harrowfield, D. L. Kepert, J. M. Patrick, and A. H. White, Aust. J. Chem. **36**, 483 (1983).
[25] A. V. Astashkin, A. M. Raitsimring, and P. Caravan, J. Phys. Chem. A **108**, 1990 (2004).
[26] A. V. Astashkin, A. M. Raitsimring, D. Baute, D. Goldfarb, and P. Caravan, J. Phys. Chem. A **108**, 7318 (2004).
[27] A. E. Reed, R. B. Weinstock, and F. Weinhold, J. Chem. Phys. **83**, 735 (1985).
[28] E. Clark, J. Chem. Theory Comput. **4**, 708 (2008).
[29] S. Xantheas, J. Chem. Phys. **104**, 8821 (1996).
[30] K. E. Gutowski and D. A. Dixon, J. Phys. Chem. A **110**, 8840 (2006).
[31] C. J. Cramer, *Essentials of Computational Chemistry: Theories and Models*, 2nd Edn., Chichester, UK: Wiley, 355 (2004).
[32] S. G. Bratsch and J. J. Lagowski, J. Phys. Chem. **89**, 3317 (1985).

DOI:10.1088/1674-0068/22/04/395-400